

11-1-2020

Palmitic acid induces inflammation in placental trophoblasts and impairs their migration toward smooth muscle cells through plasminogen activator inhibitor-1

Amanda M. Rampersaud
Western University

Caroline E. Dunk
Sinai Health System

Stephen J. Lye
Sinai Health System

Stephen J. Renaud
Western University, srenaud4@uwo.ca

Follow this and additional works at: <https://ir.lib.uwo.ca/paedpub>

Citation of this paper:

Rampersaud, Amanda M.; Dunk, Caroline E.; Lye, Stephen J.; and Renaud, Stephen J., "Palmitic acid induces inflammation in placental trophoblasts and impairs their migration toward smooth muscle cells through plasminogen activator inhibitor-1" (2020). *Paediatrics Publications*. 2284.
<https://ir.lib.uwo.ca/paedpub/2284>

Palmitic acid induces inflammation in placental trophoblasts and impairs their migration toward smooth muscle cells through plasminogen activator inhibitor-1

Amanda M. Rampersaud¹, Caroline E. Dunk², Stephen J. Lye^{2,3}, and Stephen J. Renaud^{1,4,*}

¹Department of Anatomy and Cell Biology, Schulich School of Medicine and Dentistry, University of Western Ontario, London, ON, Canada ²Research Centre for Women's and Infants' Health, Lunenfeld-Tanenbaum Research Institute, Sinai Health System, Toronto, ON, Canada ³Department of Obstetrics and Gynecology, Faculty of Medicine, University of Toronto, Toronto, ON, Canada ⁴Children's Health Research Institute, Lawson Health Research Institute, London, ON, Canada

*Correspondence address. Department of Anatomy and Cell Biology, University of Western Ontario, 1151 Richmond St, London, ON N6A5C1, Canada. Tel: +1-519-661-2111, ext: 88272; Fax: +1-519-661-3936; E-mail: srenaud4@uwo.ca

<https://orcid.org/0000-0001-7257-5354>

Submitted on March 05, 2020; resubmitted on August 21, 2020; editorial decision on August 28, 2020

ABSTRACT: A critical component of early human placental development includes migration of extravillous trophoblasts (EVTs) into the decidua. EVT migration toward and displacement of vascular smooth muscle cells (SMCs) surrounding several uterine structures, including spiral arteries. Shallow trophoblast invasion features in several pregnancy complications including preeclampsia. Maternal obesity is a risk factor for placental dysfunction, suggesting that factors within an obese environment may impair early placental development. Herein, we tested the hypothesis that palmitic acid, a saturated fatty acid circulating at high levels in obese women, induces an inflammatory response in EVT that hinders their capacity to migrate toward SMCs. We found that SMCs and SMC-conditioned media stimulated migration and invasion of an EVT-like cell line, HTR8/SVneo. Palmitic acid impaired EVT migration and invasion toward SMCs, and induced expression of several vasoactive and inflammatory mediators in EVT, including endothelin, interleukin (IL)-6, IL-8 and PAI1. PAI1 was increased in plasma of women with early-onset preeclampsia, and PAI1-deficient EVT were protected from the anti-migratory effects of palmitic acid. Using first trimester placental explants, palmitic acid exposure decreased EVT invasion through Matrigel. Our findings reveal that palmitic acid induces an inflammatory response in EVT and attenuates their migration through a mechanism involving PAI1. High levels of palmitic acid in pathophysiological situations like obesity may impair early placental development and predispose to placental dysfunction.

Key words: extravillous trophoblasts / smooth muscle cells / obesity / palmitic acid / plasminogen activator inhibitor-1 / cell migration

Introduction

Extravillous trophoblast (EVT) invasion is a critical component of human placentation. EVT arise at the distal tips of large anchoring villi and proliferate extensively to form stratified cell columns. A subpopulation of EVT then acquires invasive properties, accompanied by expression of human leukocyte antigen-G (HLA-G), integrin $\alpha 1$ (ITGA1) and human epidermal growth factor receptor 2 (HER2) (Damsky *et al.*, 1994; Wright *et al.*, 2010). These EVT invade into the decidua as far as the inner third of the myometrium, anchor the placenta to the uterus, integrate into various uterine structures (including

endometrial glands and blood vessels) and transform the tissue architecture of the maternal-placental interface (Moser *et al.*, 2018). Migrating EVT displace smooth muscle cells (SMCs) surrounding uterine spiral arteries (Whitley and Cartwright, 2009; James *et al.*, 2012), transforming these vessels into low-resistance conduits capable of providing the placenta with a consistent supply of maternal blood that gently bathes the delicate surfaces of the chorionic villi. Defects in EVT migration cause shallow spiral artery remodeling and are linked to serious pregnancy complications including preeclampsia, which is a major cause of maternal and fetal sickness and mortality (Lyall *et al.*, 2013).

Maternal obesity is a major risk factor for placental dysfunction and various obstetric complications (Leddy *et al.*, 2008; Lynch *et al.*, 2008; Roberts *et al.*, 2011; Åmark *et al.*, 2018). A study evaluating depth of spiral artery remodeling in stillbirths found that elevated BMI was the only maternal characteristic that significantly associated with poor spiral artery remodeling (Avagliano *et al.*, 2012). In rats, a species that, like humans, relies on deep trophoblast invasion for pregnancy success, diet-induced obesity impairs trophoblast migration and spiral artery remodeling, and triggers placental inflammation (Hayes *et al.*, 2014). Therefore, factors within an obesogenic milieu may impact early aspects of placental development, such as EVT invasion, and predispose to adverse pregnancy outcomes.

Obesity is associated with elevated plasma levels of free fatty acids (Jensen *et al.*, 1989; Boden, 2008). In particular, plasma levels of saturated long-chain fatty acids such as palmitic acid are higher in individuals with elevated BMI (Yew Tan *et al.*, 2015), including pregnant women with elevated pre-pregnancy BMI or excessive gestational weight gain (Vidakovic *et al.*, 2015). Palmitic acid is the most common saturated fatty acid in the human body. It has a sixteen-carbon backbone (16:0) and is obtained through dietary intake or synthesized endogenously from other macronutrients. High levels of palmitic acid modulate cellular metabolism and promote production of inflammatory mediators in several cell-types (Gupta *et al.*, 2012; Zhou *et al.*, 2013; Tian *et al.*, 2015; Sergi *et al.*, 2018; Korbecki and Bajdak-Rusinek, 2019). In primary cytotrophoblasts isolated from term placentas, palmitic acid (and stearic acid, another long-chain saturated fatty acid) activates toll-like receptor 4 and stimulates production of pro-inflammatory cytokines including tumor necrosis factor alpha, interleukin (IL)-6 and IL-8 (Yang *et al.*, 2015). These effects are not observed in cytotrophoblasts exposed to unsaturated fatty acids, indicating that saturated fatty acids such as palmitic acid may be uniquely capable of promoting inflammation at the maternal-placental interface. In some cell-types, palmitic acid also induces expression of plasminogen activator inhibitor-1 (PAI1) (Jeong *et al.*, 2016), a serine protease inhibitor and powerful regulator of hemostasis, fibrinogenesis and cell migration. PAI1 inhibits EVT motility *in vitro*, and levels of PAI1 are elevated in pregnancy complications characterized by deficient placentation (e.g. preeclampsia and unexplained recurrent pregnancy loss) (Ye *et al.*, 2017). Since excessive inflammation and production of PAI1 is associated with compromised trophoblast function and predisposes to poor placentation (Challier *et al.*, 2008; Renaud *et al.*, 2011; Cotechini and Graham, 2015; Baines *et al.*, 2020), herein we hypothesize that palmitic acid stimulates expression of PAI1 and other inflammatory mediators in EVTs, and reduces their migratory potential.

In this study, we investigated the effect of SMCs on EVT migration, using co-cultures of vascular SMCs with a well-established EVT-like cell-line as a model system. Next, we determined whether palmitic acid affects migration of EVTs toward SMCs, and we profiled expression of inflammatory mediators, including PAI1, by EVTs following exposure to palmitic acid. We found that palmitic acid stimulates inflammatory pathways in EVTs and impairs their migratory potential. Moreover, we identified PAI1 as a central mediator of the anti-migratory effects of palmitic acid. Our results suggest that high levels of palmitic acid in susceptible individuals may contribute to a suboptimal maternal-placental interface and predispose to deficient placentation.

Methods

Cells

HTR8/SVneo cells (henceforth called HTR8 EVTs), a well-established human first trimester invasive EVT-like cell-line derived from placental explant outgrowths (Graham *et al.*, 1993), were maintained in standard culture conditions (37°C, 5% CO₂) with RPMI-1640 medium containing 5% fetal bovine serum (FBS), 100 units/ml penicillin and 100 µM streptomycin (Sigma-Aldrich) for no more than 20 sequential passages. The number of viable HTR8 EVTs was assessed by staining with trypan blue and counting with a hemocytometer.

Primary SMCs derived from human aorta (Cell Applications 354-05a) were maintained in proprietary growth media (Cell Applications 311-500). Cells were plated at a density of 1.5×10^4 cells/cm², and grown in standard culture conditions for up to 15 passages. To differentiate cells to a contractile phenotype, 1.0×10^4 SMCs/cm² were plated, and growth medium was replaced with SMC differentiation medium (Cell Applications 311D-250) for up to 7 days. To produce SMC-conditioned media, SMCs were differentiated for 5 days, then new differentiation medium was provided and conditioned for 48 h. Conditioned media were then removed, centrifuged and used for experiments.

Primary human uterine microvascular endothelial cells (PromoCell C-12295) were maintained in proprietary growth media (PromoCell C-22020). Cells were plated at a density of 2.0×10^4 cells/cm² and grown in standard culture conditions for up to 10 passages.

Human embryonic kidney (HEK)-293T cells were maintained in standard culture conditions with Dulbecco's Modified Eagle's Medium (DMEM) containing 10% FBS, 100 units/ml penicillin and 100 µM streptomycin for up to 20 passages.

Tissue collection and culture

Informed written consent was obtained from each patient in accordance with the Declaration of Helsinki. Collections were approved by the Morgentaler Clinic and the Mount Sinai Hospital Research Ethics Board (Toronto, Canada; REB12-0007E).

For collection of plasma, blood samples were procured from healthy non-pregnant women, pregnant women during mid-second trimester (15.2–17.2 weeks), and third-trimester pregnant women with or without early-onset preeclampsia. Clinical measures of patients are provided in Table 1. Blood samples were collected in sterile tubes containing ethylenediaminetetraacetic acid-dipotassium salt, and plasma was immediately separated from peripheral blood mononuclear cells and polymorphonuclear leukocytes using a dual density gradient separation kit (Histopaque 1119/1077, Sigma-Aldrich), according to the manufacturer's protocol. Plasma was aliquoted and stored at –80°C until use.

First trimester (5–8 weeks) placentas, obtained at the time of elective terminations of pregnancy, were used to prepare placental explants as previously described (Nadeem *et al.*, 2011). Villous explants were dissected, washed in PBS and embedded on culture inserts (0.4-µm pores, 12-mm diameter; EMD Millipore) precoated with 0.2 ml undiluted phenol red-free Matrigel (Becton-Dickinson). Inserts were placed into wells containing serum-free DMEM/F12 media containing 100 U/ml penicillin/streptomycin, 2 mM L-glutamine, 100 µg/ml gentamicin and 2.5 µg/ml fungizone and were incubated at

Table 1 Clinical measures of patients used for quantification of PAII levels in plasma.

Demographic	Non-pregnant (n = 6)	Second trimester (n = 10)	Third trimester No preeclampsia (n = 9)	Third trimester Preeclampsia (n = 8)
Age (years)				
Mean	32.43	32.52	29.86	26.88
Range	25–37	20–42	23–40	25–35
Parity				
Nullipara	3	5	5	6
Multipara	3	5	3	2
Gestational age at blood collection (weeks)				
Mean	Not applicable	16.33	27.80	29.53
Range		15.2–17.2	26.0–29.0	27–34.0
Gestational age at delivery (weeks)				
Mean	Not applicable	38.07	39.00	31.20*
Range		37–41.1	37.3–40.6	28.2–34.4
Max systolic blood pressure	Not measured	116.6 ± 11.93	124.2 ± 19.83	154.79 ± 6.24*
Max diastolic blood pressure	Not measured	71 ± 7.65	72.1 ± 9.89	100.33 ± 7.72*

*P < 0.05.

37°C with an atmosphere containing 3% O₂ and 5% CO₂. After 48 h plating, adherent explants that initiated EVT outgrowths were given SMC-conditioned media containing either bovine serum albumin (BSA) or 125 μM palmitic acid for 72 h. Outgrowth area was measured using Image J software (Schneider et al., 2012). Each treatment was conducted in triplicate and repeated using explants from six different placentas. To determine depth of EVT invasion, the Matrigel plug (containing invaded EVTs) was fixed in 4% paraformaldehyde, embedded in paraffin and 5-μm serial sections prepared. Sections were rehydrated and stained using hematoxylin and eosin to identify invading EVTs. The depth of EVT invasion into Matrigel was then calculated based on the number of consecutive sections in which EVTs were detected.

Treatments

To prepare fatty acids, 30% fatty acid-free BSA was conjugated 2:1 to either 20 mM palmitic acid or oleic acid and added to SMC-conditioned media at final concentrations of 125, 250 and 500 μM (Sigma-Aldrich). Controls consisted of medium containing an equivalent amount of BSA. Activity of P38-MAPK was inhibited using 10 μM SB203580 (P38-MAPK inhibitor) dissolved in dimethyl sulfoxide (DMSO). SMC-conditioned media containing DMSO was used as control for these experiments.

Immunofluorescence

Cells were fixed with 4% paraformaldehyde, permeabilized using 0.3% Triton X-100, blocked in 10% normal goat serum (ThermoFisher Scientific), and immersed in antibodies targeting α-smooth muscle actin (A2547, 1:400, Sigma Aldrich), calponin (D8L2T, 1:50, Cell Signaling Technology) or transgelin (sc-53932, 1:50, Santa Cruz Biotechnology).

Cells were then incubated with species-appropriate fluorescent antibodies (AlexaFluor, ThermoFisher Scientific), and nuclei counterstained using 4',6-diamidino-2-phenylindole (DAPI, ThermoFisher Scientific). Cells were imaged using a Zeiss Axio fluorescence microscope.

5-Ethynyl-2'-deoxyuridine incorporation assay

HTR8 EVTs were seeded onto Poly-D lysine-coated coverslips at 5×10^4 cells/coverslip. The following day, 10 μM 5-ethynyl-2'-deoxyuridine (EdU, dissolved in culture media) was added to cells for 4 h. Cells were fixed using 4% paraformaldehyde and detection of EdU was performed according to the manufacturer's instructions (ClickIT EdU Proliferation Kit, ThermoFisher Scientific). Nuclei were detected using Hoechst. Cells were imaged with a Zeiss Axio fluorescence microscope. The total number of cells and number of EdU-positive cells were counted in three random non-overlapping fields of view per well, and the percentage of EdU-positive cells was calculated.

Cell viability and apoptosis assays

HTR8 EVTs were seeded at 5×10^4 cells/cm². The following day, SMC-conditioned media containing BSA, palmitic acid or oleic acid were added for 24 h. As a positive control, 10 μM camptothecin (Cell Signaling Technology) was added to cells for 24 h. Cells were then trypsinized, centrifuged and incubated with annexin V and propidium iodide (PI) as per the manufacturer's instructions (Early Apoptosis Detection Kit, Cell Signaling Technology). Cells were analyzed by flow cytometry using a BD FACSCanto cell analyser (BD Biosciences). Data were analyzed using FlowJo software. Gating strategies can be found in [Supplementary Fig. S1](#). In brief, gating commenced with a forward scatter area versus forward scatter height plot to remove doublets,

followed by a second gate on forward scatter area versus side scatter area to remove obvious debris from the plot while retaining both live and dead cells. Single-stained positive control cells on annexin V versus PI plots were gated on this population, which was also used to derive the frequencies shown in Fig. 3.

Transwell migration and invasion assays

To measure cell migration, 2.0×10^4 HTR8 EVT cells were placed into transwell inserts (8- μ m pore, 6.5-mm diameter, Greiner BioOne). Media containing 3.8×10^4 human uterine microvascular endothelial cells, 1.9×10^4 synthetic SMCs, 1.9×10^4 contractile SMCs or conditioned media from contractile SMCs containing either fatty acids or inhibitors (see cell treatments) were added to the lower chamber. Cells were incubated in standard culture conditions for 24 h. Cells in the upper portion of the transwell were removed with a cotton swab. Cells attached to the underside of the membrane were fixed in methanol, then stained with Diff-Quik cytometry stain (GE Healthcare). Membranes were excised, placed onto slides and counted using a bright-field microscope. Normalized migration indices were calculated by dividing the number of cells that migrated under both control and treatment conditions by the mean number of cells that migrated in control conditions, as done previously (Jeyarajah *et al.*, 2019). This normalization step was performed to determine the relative change in cell migration for each experiment, which facilitated comparisons between experiments.

Cell invasion was assessed by precoating transwells with growth factor-reduced Matrigel (BD Biosciences, 400 μ g/ml diluted in serum-free RPMI-1640) for 3 h. Medium was removed, and then 4.0×10^4 HTR8 EVT cells were placed on top of the Matrigel. All other steps were the same as described above. Normalized invasion indices were determined by dividing the number of cells that invaded under both control and treatment conditions by the mean number of cells that invaded in control conditions.

Immunohistochemistry

Explants were fixed in 4% paraformaldehyde, embedded in paraffin and sectioned at 5- μ m thickness. Sections were deparaffinized, rehydrated and subjected to heat-mediated antigen retrieval in 10 mM citrate buffer pH 6.0. Sections were then immersed in 0.1% Sudan Black in 70% ethanol for 1 min to reduce autofluorescence, blocked and immersed in primary antibodies specific for: proliferating EVT markers, i.e. proliferating cell nuclear antigen (PCNA; sc-56, 1:200, Santa Cruz Biotechnology), Ki67 (ab15580, 1:200, Abcam) and integrin α 5 (ITGA5; ab112183, 1:1000, Abcam); or markers of invasive EVTs, i.e. ITGA1 (ab243032, 1:500, Abcam), HLAG (sc-21799, 1:50, Santa Cruz Biotechnology) and HER2 (A0485, 1:300, Dako). Primary antibodies were diluted in PBS and were applied to sections overnight at 4°C. The following day, species-appropriate fluorescent antibodies were applied (AlexaFluor, ThermoFisher Scientific), and DAPI was used to counterstain nuclei. Sections were mounted with Fluoromount-G (SouthernBiotech), and images acquired using either a Nikon DS-Qi2 microscope or a Quorum Wave FX spinning disc confocal system comprising a Leica DMI 6000B microscope with a Yokogawa Spinning Head and Image EM Hamamatsu EMCCD camera and Velocity imaging software. To ensure fair comparison between control and treatment in the explant experiments, control images were initially

captured and time of exposure and laser intensity recorded and set. Treatment images were then captured using the same settings.

Western blot analysis

Cells were lysed using 1 \times Laemmli sample buffer (2% sodium dodecyl sulfate, 10% glycerol, 5% 2-mercaptoethanol, 0.002% bromophenol, 0.125 M Tris-HCl and 0.5 M dithiothreitol) supplemented with phenylmethylsulfonyl fluoride, boiled and loaded onto sodium dodecyl sulfate-containing polyacrylamide gels. Proteins were separated using gel electrophoresis and transferred to polyvinylidene difluoride membranes (GE Healthcare). Membranes were blocked with 3% BSA in TBS containing 0.1% Tween-20 and probed using antibodies targeting α -smooth muscle actin (A2547, 1:2000, Sigma Aldrich), calponin (D8L2T, 1:1000, Cell Signaling Technology), transgelin (SC-53932, 1:500, Santa Cruz Biotechnology), P38-MAPK (D13E1, 1:1000, Cell Signaling Technology), phosphorylated P38-MAPK (D3F9, 1:1000, Cell Signaling Technology), ERK1/2 (9102, 1:1000, Cell Signaling Technology) or phosphorylated ERK1/2 (E10, 1:2000, Cell Signaling Technology). Expression of α -tubulin (CP06, 1:1000, Calbiochem) was used as a loading control. Proteins were detected using a LI-COR Odyssey imaging system (LI-COR Biosciences) following incubation with species-appropriate, infrared-conjugated secondary antibodies (Cell Signaling Technology).

Taqman PCR array and quantitative RT-PCR

RNA was extracted using TriZol (ThermoFisher Scientific). The aqueous phase was diluted 1:1 with 70% ethanol, placed on RNeasy columns (Qiagen), treated with DNase I, and purified. Complementary DNA was generated from purified RNA using High Capacity Reverse Transcription kit (ThermoFisher Scientific), diluted 1:10, and used for quantitative RT-PCR (qRT-PCR). Relative mRNA levels of a panel of inflammation-associated genes were initially screened using a Human Immune Taqman PCR array (4418718, ThermoFisher Scientific) and Taqman Fast Advanced Master Mix. A CFX Connect Real-Time PCR system (Bio-Rad Laboratories) was used for amplification and fluorescence detection. The cycling conditions included an initial uracil-N-glycosylase step (50°C for 2 min), followed by enzyme inactivation (95°C for 20 s), and then 40 cycles of two-step PCR (95°C for 1 s then 60°C for 20 s). Four reference genes (*18S*, *GAPDH*, *HPRT1* and *GUSB*) were also analyzed in the array, and their expressions were stable among the conditions tested. Transcript levels of select genes (*EDNI*, *IL6*, *LIF*, *IL1A*, *PTGS2* and *VEGFA*) were validated on independent samples using qRT-PCR with predesigned Taqman probes (ThermoFisher Scientific, Table II) and *18S* as a reference RNA. All other qRT-PCR analyses were conducted using cDNA mixed with SensiFAST SYBR Green PCR Master Mix (FroggaBio) and primers described in Table III. Cycling conditions included an initial holding step (95°C for 3 min), followed by 40 cycles of two-step PCR (95°C for 10 s, 60°C for 45 s), then a dissociation step (65°C for 5 s, and a sequential increase to 95°C). Relative mRNA expression was calculated using the comparative cycle threshold ($\Delta\Delta$ Ct) method, using *18S* as a reference RNA.

Enzyme immunoassay

Levels of PAII in human plasma were measured using a Bio-Plex multiplex enzyme immunoassay (Customized Human Cancer Biomarker Assay, Bio-Rad Laboratories). Plasma was diluted 1:4 in assay diluent prior to performing the assay. Levels of PAII in media conditioned by HTR8 EVT cells were measured using a Human Total PAII enzyme immunoassay (DY9387-05, Biotechne), as per the manufacturer's instructions. A standard curve was generated using absorbance values plotted against defined concentrations of recombinant PAII. Conditioned media were diluted in assay buffer to ensure absorbance values fell within the linear range of the standard curve.

Lentivirus production

Lentivirus-encapsulated short hairpin RNAs (shRNAs) were generated to knockdown *SERPINE1* gene expression. Briefly, HEK-293T cells were transfected using Lipofectamine 2000 (ThermoFisher Scientific) with lentiviral packaging plasmids (MD2.G, MDLG/RRE, and RSV-Rev) and a *SERPINE1* shRNA construct encoded in a PLKO.1 vector (henceforth called shPAII: TRCN0000370159, sense: ACACCCTCAGCATGTTTCATTG; Sigma-Aldrich). A control PLKO.1 vector containing a scrambled shRNA (Addgene 1864) was used as a control. Lentivirus-containing culture supernatants were collected at 24 h and 48 h and stored at -80°C until use. To transduce HTR8 EVTs, cells were exposed to lentiviral particles for 24 h in the presence of $8\ \mu\text{g/ml}$ hexadimethrine bromide, as described previously (Jaju Bhattad et al., 2020). After 48-h infection, transduced cells were selected with puromycin ($3.5\ \mu\text{g/ml}$).

Table II Taqman probe IDs.

Gene name	Assay ID	Amplicon size
<i>EDN1</i>	Hs00174961_m1	62 bp
<i>IL1A</i>	Hs00174092_m1	69 bp
<i>IL6</i>	Hs00174131_m1	95 bp
<i>LIF</i>	Hs00171455_m1	66 bp
<i>VEGFA</i>	Hs00173626_m1	77 bp
<i>PTGS2</i>	Hs00153133_m1	75 bp
<i>RNA18SN5</i>	Hs99999901_s1	187 bp

bp, base pairs.

Statistical analysis

Statistical comparisons between two means were tested using Student's *t*-test; statistical comparisons between three or more means were assessed using analysis of variance, followed by Tukey's *post hoc* analysis. A two-way ANOVA followed by a Sidak's multiple comparison test was performed to compare HTR8 EVTs transduced with shRNAs and then exposed to BSA or palmitic acid. Means were considered statistically different when $P < 0.05$. GraphPad Prism 7.0 was used for all graphing and statistical analysis. The Human Immune PCR array was conducted using one replicate; all other experiments were repeated at least three independent times. The specific number of replicates is indicated in the figure legends.

Results

SMCs stimulate EVT migration and invasion

EVTs migrate chemotactically toward several uterine structures containing vascular SMCs. Therefore, to determine whether SMCs drive migration of EVTs, human vascular SMCs were first differentiated to a contractile phenotype, reminiscent of vascular SMCs surrounding spiral arteries in first trimester human decidua. When cultured under differentiation conditions, vascular SMCs progressively increased levels of calponin, α -smooth muscle actin and transgelin and possessed morphological characteristics consistent with a contractile phenotype (Supplementary Fig. S2). We then placed uncoated or Matrigel-coated transwells harboring HTR8 EVTs into wells containing differentiated SMCs, to determine whether SMCs drive migration and invasion of EVTs (Fig. 1A). Compared to control conditions in which SMCs were absent, the presence of SMCs increased HTR8 EVT migration by 16-fold (Fig. 1B, $P = 0.0001$) and increased invasion by 2.6-fold (Fig. 1C, $P < 0.0001$). Although undifferentiated (synthetic) SMCs and human uterine microvascular endothelial cells enhanced migration of HTR8 EVTs, the extent of migration was not as robust as with differentiated SMCs (3.5-fold and 1.5-fold, respectively, $P = 0.0004$ and $P = 0.0002$, Supplementary Fig. S3).

To determine whether factors secreted by SMCs stimulated EVT migration, transwells containing HTR8 EVTs were placed into wells containing media conditioned by contractile SMCs (Fig. 1D). Compared to unconditioned media, vascular SMC-conditioned media increased HTR8 EVT migration by 7.4-fold (Fig. 1E, $P = 0.0002$), and

Table III List of primers used for qRT-PCR.

Gene Name	Accession No.	Forward primer	Reverse primer
<i>SERPINE1</i>	NM_000602.4	AAGAGGTGCCTCTCTCTGCC	TAGGGGCTTCCTGAGGTCGA
<i>CXCL8</i>	NM_000584.4	AATTCATAAAAAAATTCATT	TGGTACAATGAAAAACTATT
<i>RNA18SN5</i>	NR_003286.4	GCAATTATCCCATGAACG	GGCCTCACTAAACCATCCAA

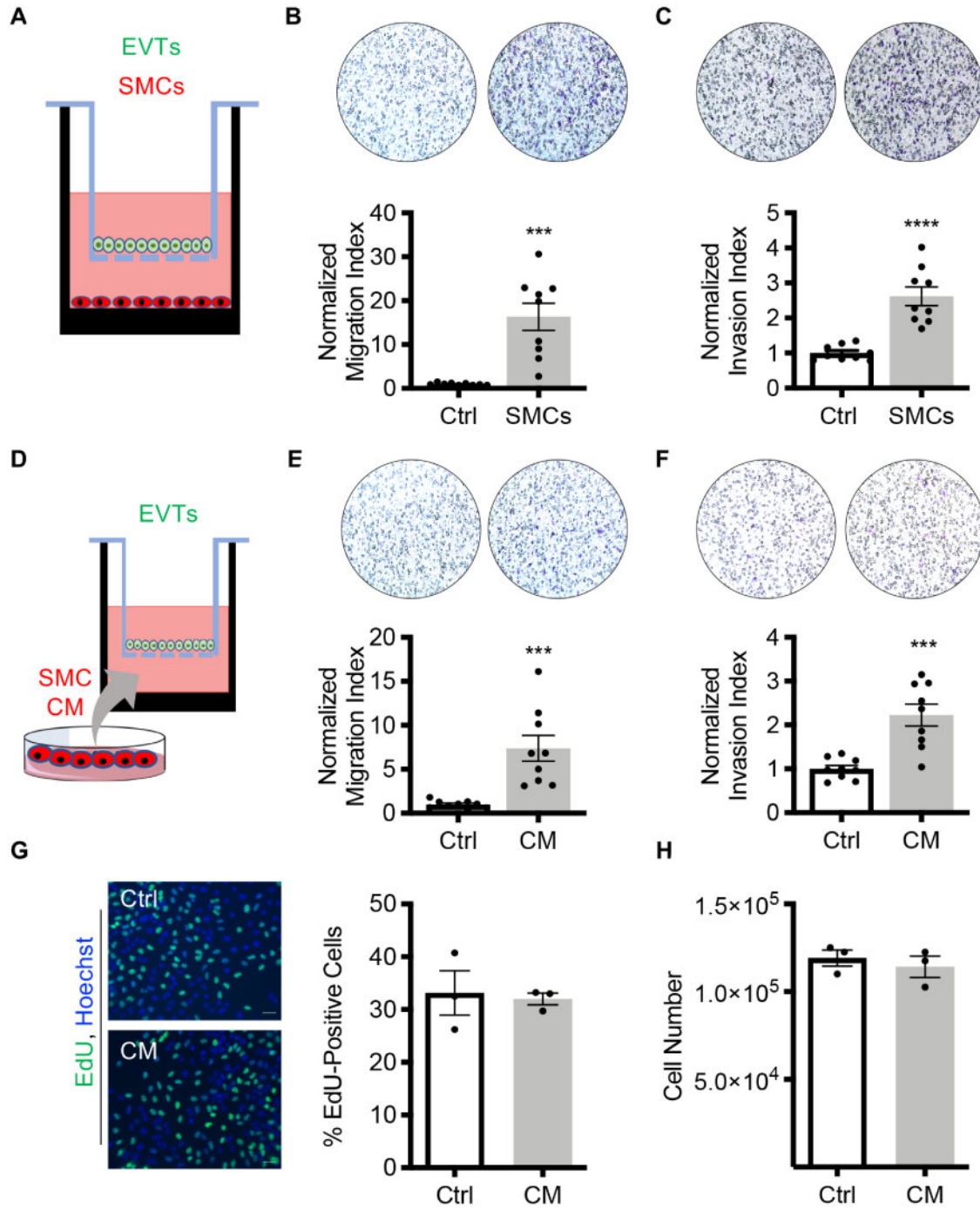


Figure 1. Contractile SMCs enhance migration and invasion of EVT. (A) Schematic of co-culture design with smooth muscle cells (SMCs). Relative number of HTR8 extravillous trophoblasts (EVTs) that migrated (B) and invaded (C) in the presence of SMCs. Controls (Ctrl) consisted of wells not containing SMCs. Representative images of membranes are included above each graph (the black circles represent pores within the transwell membrane; cells appear purple). (D) Schematic of experimental design, showing transwells containing HTR8 EVT placed into wells containing SMC-conditioned media (CM). Relative number of HTR8 EVT that migrated (E) and invaded (F) in the presence of SMC CM. Ctrl represents cells migrating toward unconditioned media. Representative images of membranes are included above each graph. (G) Percentage of EdU-positive HTR8 EVT after exposure to SMC CM in comparison to cells immersed in unconditioned media (Ctrl). Representative images are shown to the left of the graph. Nuclei were detected using Hoechst. (H) Trypan blue viability assay showing total live cell counts of HTR8 EVT exposed to SMC CM compared to Ctrl (unconditioned media). Graphs represent means ± SEM. Migration and invasion assays were conducted using three membranes per treatment from each of three independent experiments. Proliferation and viability experiments: n = 3. Asterisks denote statistical significance (**P < 0.01; ***P < 0.001; ****P < 0.0001). Scale bar = 100 μm.

increased invasion through Matrigel by 2.2-fold (Fig. 1F, $P=0.0005$). To investigate whether SMCs affect proliferation of HTR8 EVT, EdU incorporation and trypan blue viability assays were performed. There was no significant difference in the number of proliferating or viable cells cultured with SMC-conditioned media versus unconditioned media (Fig. 1G and H). These results suggest that SMCs drive migration and invasion of HTR8 EVTs, and that this effect is not due to altered cell proliferation.

SMC-conditioned media induces phosphorylation of kinases required for EVT migration

To determine whether contractile SMCs enhance phosphorylation of kinases required for migration of EVTs, we treated HTR8 EVTs with media conditioned by differentiated SMCs and assessed phosphorylation of signaling factors implicated in EVT migration. There was no change in phosphorylated levels of ERK1/2 following exposure of HTR8 EVTs to SMC-conditioned media, whereas levels of phosphorylated P38-MAPK were increased 3 h following exposure to SMC-conditioned media (Fig. 2B, $P=0.007$). Total levels of these kinases were consistent among all treatment conditions. Addition of SB203580 (P38-MAPK inhibitor) to SMC-conditioned media resulted in an 84% decrease in HTR8 EVT migration compared to vehicle control (Fig. 2C, $P<0.0001$). These results suggest that P38-MAPK signaling is involved, at least in part, in vascular SMC-induced HTR8 EVT migration.

Palmitic acid inhibits EVT migration and invasion

Serum levels of palmitic acid are elevated in obese pregnancies, which are associated with poor EVT-directed spiral artery remodeling. Therefore, we next determined whether palmitic acid affects SMC-induced HTR8 EVT migration and invasion. In preliminary experiments, EVT viability was compromised following exposure to 250 μ M and 500 μ M palmitic acid (not shown), but not following exposure to 125 μ M palmitic acid, so a dose of 125 μ M palmitic acid was used for all subsequent experiments. Addition of palmitic acid to SMC-conditioned media resulted in a 91% decrease in HTR8 EVT migration and a 57% decrease in HTR8 EVT invasion, compared to cells exposed to BSA (Fig. 3, $P<0.0001$ for both). To determine if these effects were due to the bioactive properties of palmitic acid, we included an additional treatment group in which 125 μ M oleic acid (an unsaturated fatty acid) was added to media conditioned by SMCs. Addition of oleic acid had no effect on the capacity of HTR8 EVTs to migrate or invade (Fig. 3A and B). To confirm that 125 μ M palmitic acid or oleic acid did not affect viability of HTR8 EVTs, annexin V and PI expression were determined by flow cytometry. The number of apoptotic (annexin V and PI-positive) and necrotic (PI-positive) cells did not significantly differ between HTR8 EVTs exposed for 24 h to 125 μ M palmitic acid, oleic acid or BSA. In contrast, exposure of HTR8 EVTs to camptothecin caused a much higher percentage of cells to be apoptotic and necrotic (Fig. 3C, $P=0.01$ and $P=0.001$, respectively). These results demonstrate that palmitic acid impairs SMC-induced migration and invasion of HTR8 EVTs through a mechanism not involving decreased cell viability.

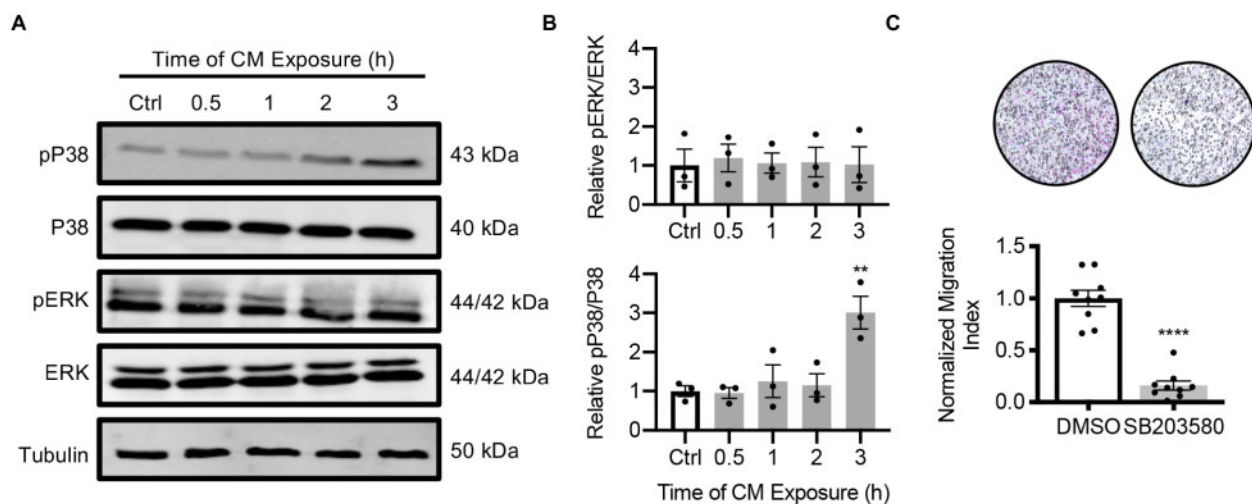


Figure 2. SMCs induce phosphorylation of P38-MAPK in EVTs. (A) Western blots depicting phosphorylated and total levels of P38-MAPK and ERK1/2 in HTR8 EVTs following exposure to SMC-conditioned medium (CM) for 0.5, 1, 2 or 3 h. Cells not exposed to CM were used as a control (Ctrl). α -tubulin was used as a loading control. Uncropped images of the western blots are provided in [Supplementary Fig. S5](#). (B) Densitometric analysis of phosphorylated ERK1/2 (pERK) and phosphorylated P38-MAPK (pP38) relative to total ERK1/2 and P38-MAPK, respectively. (C) Relative number of HTR8 EVTs that migrated toward SMC CM containing SB203580 (P38-MAPK inhibitor) in comparison to media containing dimethyl sulfoxide (DMSO). Representative images of membranes are shown above each graph (the black circles represent pores within the transwell membrane; cells appear purple). Graphs represent means \pm SEM. Western blots: $n=3$ independent experiments; migration assays were conducted using three membranes per treatment from each of three independent experiments. Asterisks denote statistical significance (** $P<0.01$; **** $P<0.0001$).

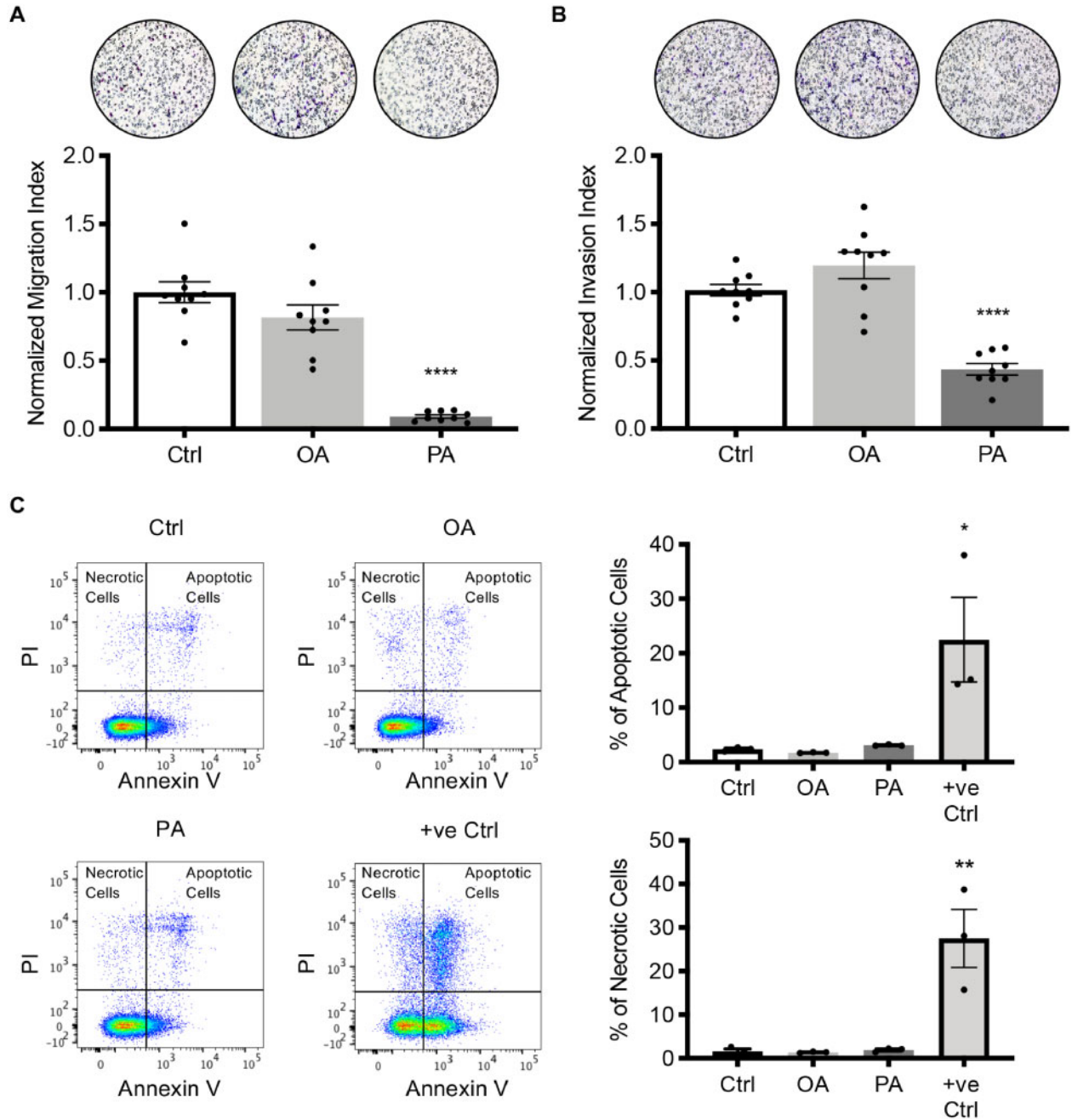


Figure 3. Palmitic acid attenuates SMC-induced EVT migration and invasion. Relative number of HTR8 EVT that (A) migrated or (B) invaded through Matrigel in the presence of SMC-conditioned media containing either 125 μ M oleic acid (OA) or 125 μ M palmitic acid (PA). Controls (Ctrl) consisted of cells migrating or invading toward SMC-conditioned media containing bovine serum albumin (BSA). Representative images of membranes are included above each graph (the black circles represent pores within the transwell membrane; cells appear purple). (C) Flow cytometry analysis of annexin V and PI-positive (apoptotic) and PI-positive (necrotic) HTR8 EVT treated with BSA (Ctrl), OA, PA or camptothecin (+ve Ctrl). Percentage of apoptotic and necrotic cells are shown to the right of the images. Gating strategies and single-stained controls can be found in [Supplementary Fig. S1](#). Graphs represent means \pm SEM. Migration and invasion assays were conducted using three membranes per treatment from each of three independent experiments. Flow cytometry: n = 3. Asterisks denote statistical significance (* P < 0.05; ** P < 0.01; **** P < 0.0001).

Palmitic acid induces a pro-inflammatory response in EVT

Palmitic acid promotes proinflammatory cytokine production in several cell-types (Korbecki and Bajdak-Rusinek, 2019). Therefore, to examine whether palmitic acid alters expression of inflammation-associated genes in EVT, cDNA was prepared from HTR8 EVT exposed to palmitic acid or BSA, and a PCR array was used to screen inflammation-associated genes potentially induced following palmitic acid exposure. The array included probes for four housekeeping genes and 92 distinct genes associated with inflammation. Of these, 33 inflammation-associated genes were expressed (normalized expression > 0.001) in HTR8 EVT following exposure to either BSA or palmitic acid (Fig. 4A). Expression of seven genes (*VEGFA*, encodes vascular endothelial growth factor A; *LIF*, encodes leukemia inhibitory factor; *PTGS2*, encodes cyclooxygenase 2; *END1*, encodes endothelin-1; *IL6*, encodes IL-6; *IL1A*, encodes IL-1 α ; and *CXCL8/IL8*, encodes IL-8) was increased at least 2-fold in EVT exposed to palmitic acid, so levels of these transcripts were further assessed using qRT-PCR. Palmitic acid increased expression of *VEGFA* (1.6-fold, $P=0.03$), *EDN1* (2-fold, $P=0.0003$), *IL6* (4.2-fold, $P=0.02$) and *CXCL8/IL8* (11-fold, Fig. 4B, $P=0.04$). Expression of *LIF* also appeared to be increased, although it did not reach statistical significance (4.5-fold, Fig. 4B, $P=0.056$), whereas there was no statistically significant change in *PTGS2* or *IL1A* (not shown). We additionally investigated expression of *SERPINE1*, because it encodes PAI: a key component of fibrogenic and thrombotic pathways circulating at increased levels in obese women (Mavri et al., 1999), and in women with early-onset preeclampsia (Fig. 5). *SERPINE1* transcript levels in HTR8 EVT were increased 15-fold following exposure to palmitic acid compared to controls (Fig. 4B, $P=0.008$), and levels of PAI in conditioned medium were increased by 62% (Fig. 4C, $P=0.02$). Collectively, palmitic acid enhances expression of various factors associated with inflammation and fibrinogenesis in EVT.

Knockdown of PAI rescues trophoblast migration following exposure to palmitic acid

To determine the contribution of elevated PAI levels to impaired EVT migration following palmitic acid exposure, we transduced HTR8 EVT with shRNAs targeting *SERPINE1* (shPAI). Compared to cells receiving the control shRNA, HTR8 EVT stably expressing shPAI exhibited reduced *SERPINE1* expression by 57% (Fig. 6A, $P=0.04$) and decreased PAI secretion by 75% (Fig. 6B, $P=0.006$). Cells expressing control shRNA exhibited 86% reduced migration (Fig. 6C, $P=0.0003$) and 58% reduced invasion (Fig. 6D, $P<0.0001$) in the presence of palmitic acid compared to BSA-treated conditions, which is consistent with our earlier observations. Remarkably, migration and invasion were completely unaffected following palmitic acid exposure in shPAI-expressing EVT (Fig. 6C and D, $P<0.0001$ and $P<0.0001$ compared to control shRNA-expressing EVT exposed to palmitic acid, respectively). Our results demonstrate that the anti-migratory functions of palmitic acid on EVT are due, at least in part, to elevated PAI expression.

Palmitic acid inhibits EVT differentiation in placental explants

Primary placental EVT outgrowths were used to further investigate the effects of palmitic acid on EVT cell invasion *ex vivo*. Explants can be used to recapitulate the multiple stages of EVT lineage development, including proliferative PCNA-positive proximal column EVT and invasive HLAG-positive distal column EVT (Fig. 7A). After 72 h in culture with SMC-conditioned media, EVT outgrowth extension was apparent in all explants, although those exposed to palmitic acid exhibited a 2-fold increased EVT outgrowth as compared to those exposed to BSA (Fig. 7B, $P=0.04$). However, explants exposed to palmitic acid exhibited a 35% decrease in depth of EVT invasion into Matrigel in comparison to those exposed to BSA (Fig. 7C, $P=0.01$), suggesting that palmitic acid did not affect EVT proliferation and spreading on Matrigel but impaired the invasive capacity of distal column EVT. Explants were further analyzed for markers of proliferative and invasive EVT. EVT emanating from explants exposed to SMC-conditioned media with BSA showed progressively decreased ITGA5 and increased cell surface expression of ITGA1, HLAG and HER2 characteristic of distal column invasive EVT. In contrast, EVT exposed to SMC-conditioned media containing palmitic acid showed an increase in HER2 on the cell surface but retained high levels of ITGA5 expression and reduced or aberrant (perinuclear) ITGA1 expression (Fig. 7D). Collectively, these results suggest that palmitic acid prevents the full acquisition of the invasive EVT phenotype, which may contribute to the reduced invasive capacity of EVT exposed to palmitic acid.

Discussion

EVT invasion is a critical component of normal placentation and maintenance of a healthy pregnancy. Since EVT typically migrate toward uterine structures containing smooth muscle (myometrium, uterine glands, endometrial veins, spiral arteries) (Moser et al., 2018), we first tested the hypothesis that EVT are driven to migrate toward SMC. We found that factors produced by contractile vascular SMC stimulate phosphorylation of P38-MAPK in HTR8 EVT, resulting in enhanced migration and invasion of these cells. We further show that palmitic acid restrains EVT motility and increases expression of several inflammatory factors in EVT, most notably PAI, and that the effects of palmitic acid on EVT motility are restored by reducing expression of PAI. Our results provide new insights into mechanisms of EVT migration, with important implications for pathophysiological conditions such as obesity, which are characterized by elevated levels of palmitic acid and a higher incidence of placental dysfunction.

Although EVT migrate toward many different uterine structures, the best understood paradigm is their migration toward spiral arteries. EVT home toward spiral arteries using both interstitial and endovascular routes and transform these vessels by displacing endothelial cells and SMC. Previous studies have shown that EVT and EVT cell-lines trigger SMC migration and apoptosis, indicating that EVT and SMC are capable of dynamic cellular crosstalk (Harris et al., 2006; Bulmer et al., 2012; Salomon et al., 2014). To the best of our knowledge, our study is the first to show that EVT migration is triggered by factors secreted by contractile vascular SMC. Although we did not deduce which factors produced by SMC are responsible for stimulating EVT

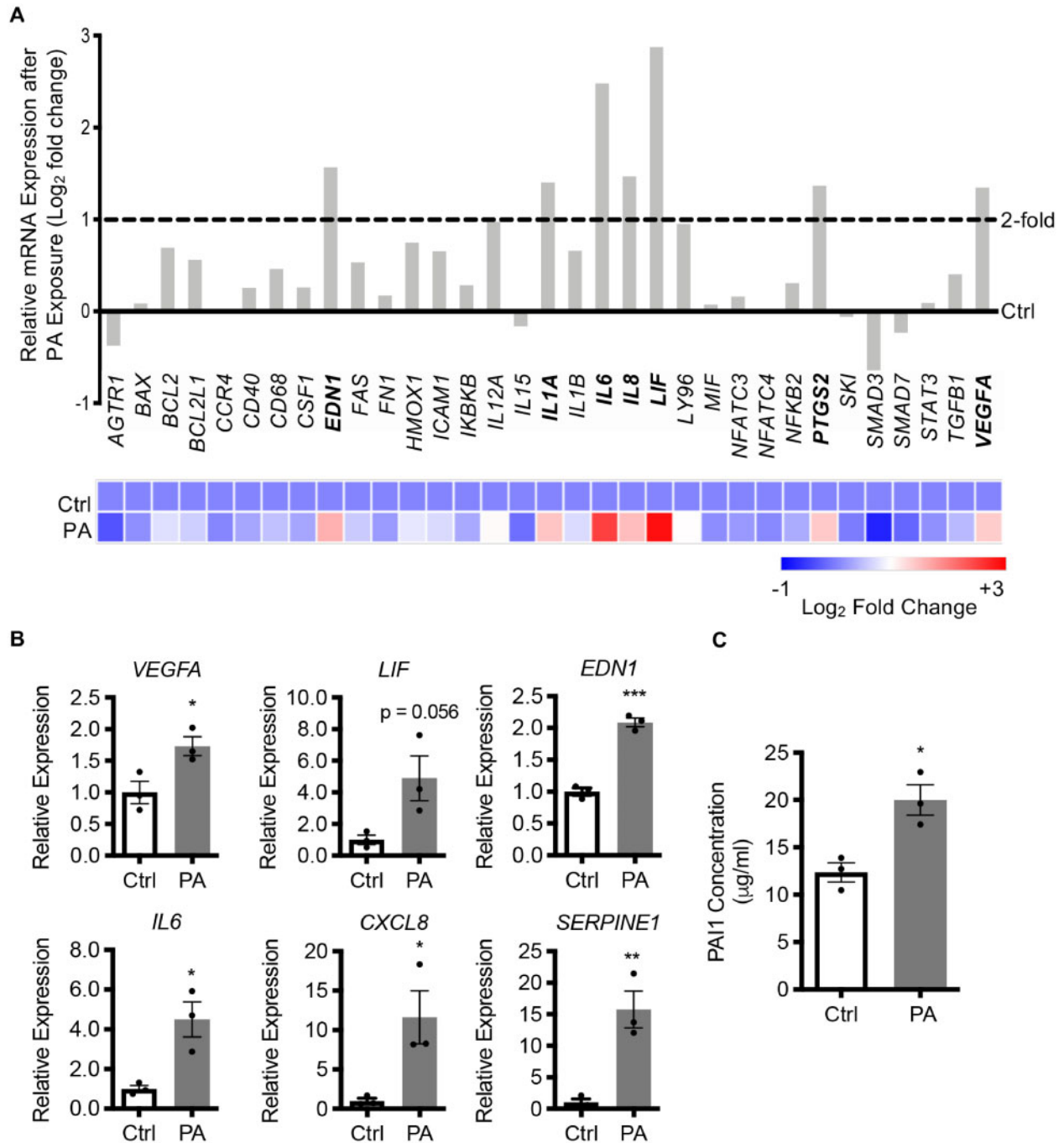


Figure 4. Palmitic acid induces production of inflammatory factors in EVT. (A) PCR array depicting transcript levels of various inflammatory factors following 24-h exposure to SMC-conditioned media containing BSA (Ctrl) or 125 µM PA. Transcript levels from Ctrl conditions are represented by the solid line. Transcripts increased >2-fold (demarcated by the dashed line) following PA exposure are bolded. A heat map is shown below the graph. (B) Transcript levels of *VEGFA*, *LIF*, *EDN1*, *IL6*, *CXCL8* and *SERPINE1* in HTR8 EVT after a 24-h exposure to SMC-conditioned media containing BSA (Ctrl) or 125 µM PA. (C) Levels of PAI1 in media conditioned by HTR8 EVT following 24-h exposure to SMC-conditioned media containing BSA (Ctrl) or 125 µM PA. Graphs in (B) and (C) represent means ± SEM based on n = 3 independent experiments. Asterisks denote statistical significance (**P* < 0.05; ***P* < 0.01; ****P* < 0.001).

migration, we did profile a select number of growth factors produced by contractile vascular SMCs (not shown), and detected high expression of platelet-derived growth factor (PDGF), epidermal growth factor (EGF) and heparin-binding EGF-like growth factor (HB-EGF). PDGF,

EGF and HB-EGF stimulate human EVT adhesion, migration and invasion (Han et al., 2010; Wright et al., 2010; Silva and Serakides, 2016; Bolnick et al., 2017), so it is possible that production of these growth factors by vascular SMCs contributes to the enhanced EVT migration observed in our study. Regardless of which factors are involved, we show that SMC-conditioned media activates P38-MAPK signaling pathways in EVTs, and inhibition of this pathway inhibits EVT migration, which is consistent with previous reports (Renaud et al., 2014).

Maternal obesity is a pregestational factor associated with a higher risk of placental dysfunction (Avagliano et al., 2011; Myatt and Maloyan, 2016). Pregnant obese women, and those with excessive gestational weight gain, have increased saturated fatty acids circulating in blood, most prominently palmitic acid (Chen et al., 2010; Vidakovic et al., 2015). Palmitic acid concentrations are normally maintained under stringent homeostatic control, likely due to its essential role in cell membrane structural properties, synthesis of palmitoylethanolamide and protein palmitoylation. Palmitic acid is metabolized in cells into saturated phospholipids (e.g. lysophosphatidylcholine), diacylglycerol and ceramides, high levels of which can alter cellular signaling events, including oxidative and endoplasmic reticulum stress and activation of protein kinase C. Palmitic acid is also a toll-like receptor agonist, and it can stimulate inflammatory responses through myeloid differentiation factor 88/nuclear factor kappa B and interferon regulatory factor 3-dependent pathways (reviewed in Korbecki and Bajdak-Rusinek (2019)). Thus, palmitic acid is a highly bioactive molecule with the potential to alter cellular gene expression, metabolism and behavior. We found that palmitic acid decreased viability of HTR8 EVTs at concentrations of 250 and 500 μM , but cell viability was unaffected at 125 μM , which is why this dose was used for our experiments. Although the

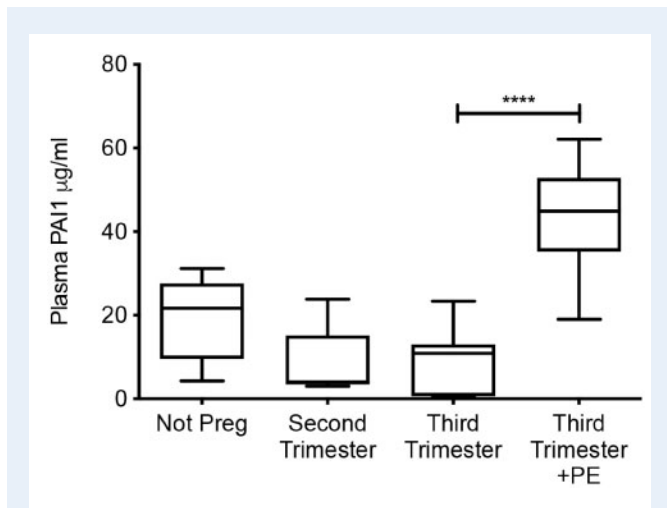


Figure 5. PAI1 is increased in plasma from women with preeclampsia. Plasma was isolated from non-pregnant women (Not Preg; $n = 6$), pregnant women in second trimester ($n = 10$) and pregnant women in early third trimester without preeclampsia ($n = 9$) or with early-onset preeclampsia (PE; $n = 8$). Levels of PAI1 in plasma were detected using a Bio-Plex Assay. Data are shown as box plots. Asterisks denote statistical significance comparing third trimester samples with and without preeclampsia (**** $P < 0.0001$).

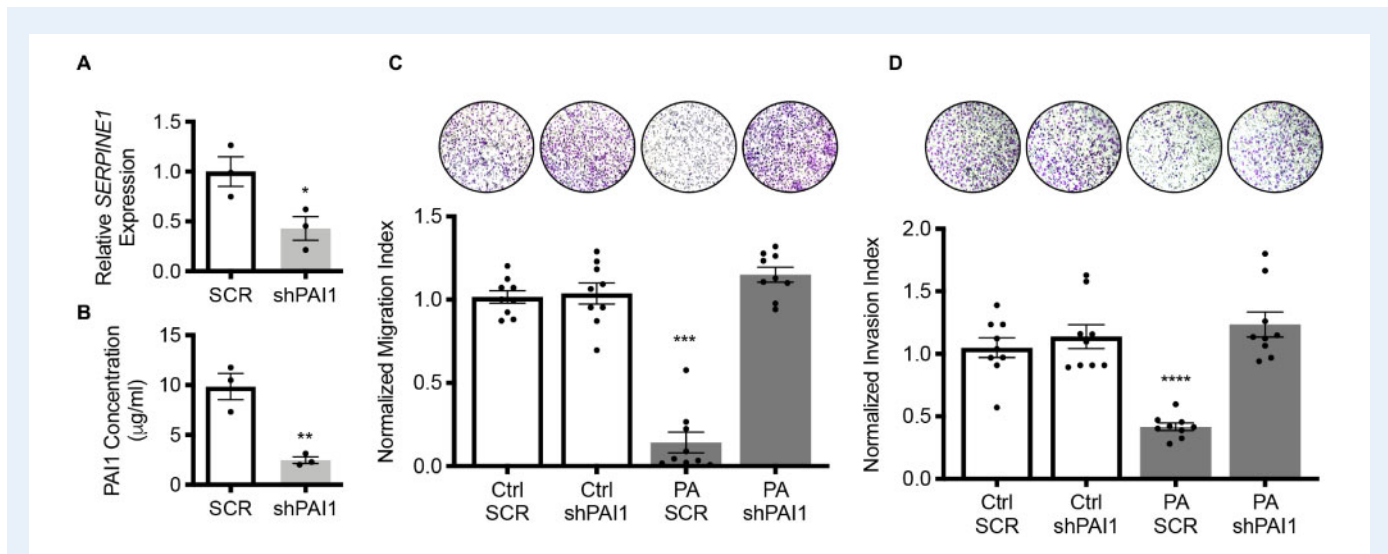


Figure 6. Knockdown of PAI1 restores EVT migration following exposure to palmitic acid. (A) Transcript levels of *SERPINE1* in HTR8 EVTs expressing shPAI1 compared to cells expressing control shRNA (scrambled; SCR). (B) Levels of PAI1 from media conditioned by HTR8 EVTs expressing SCR or shPAI1. (C and D) Relative number of HTR8 EVTs expressing SCR or shPAI1 that (C) migrated and (D) invaded toward SMC-conditioned media containing BSA (Ctrl) or PA. Representative images of membranes are shown above the graphs (the black circles represent pores within the transwell membrane; cells appear purple). Graphs represent means \pm SEM. (A) and (B) represent data from three independent experiments; (C and D) represent data obtained using three membranes per treatment from each of three independent experiments. Asterisks denote statistical significance (* $P < 0.05$, ** $P < 0.01$; *** $P < 0.001$; **** $P < 0.0001$).

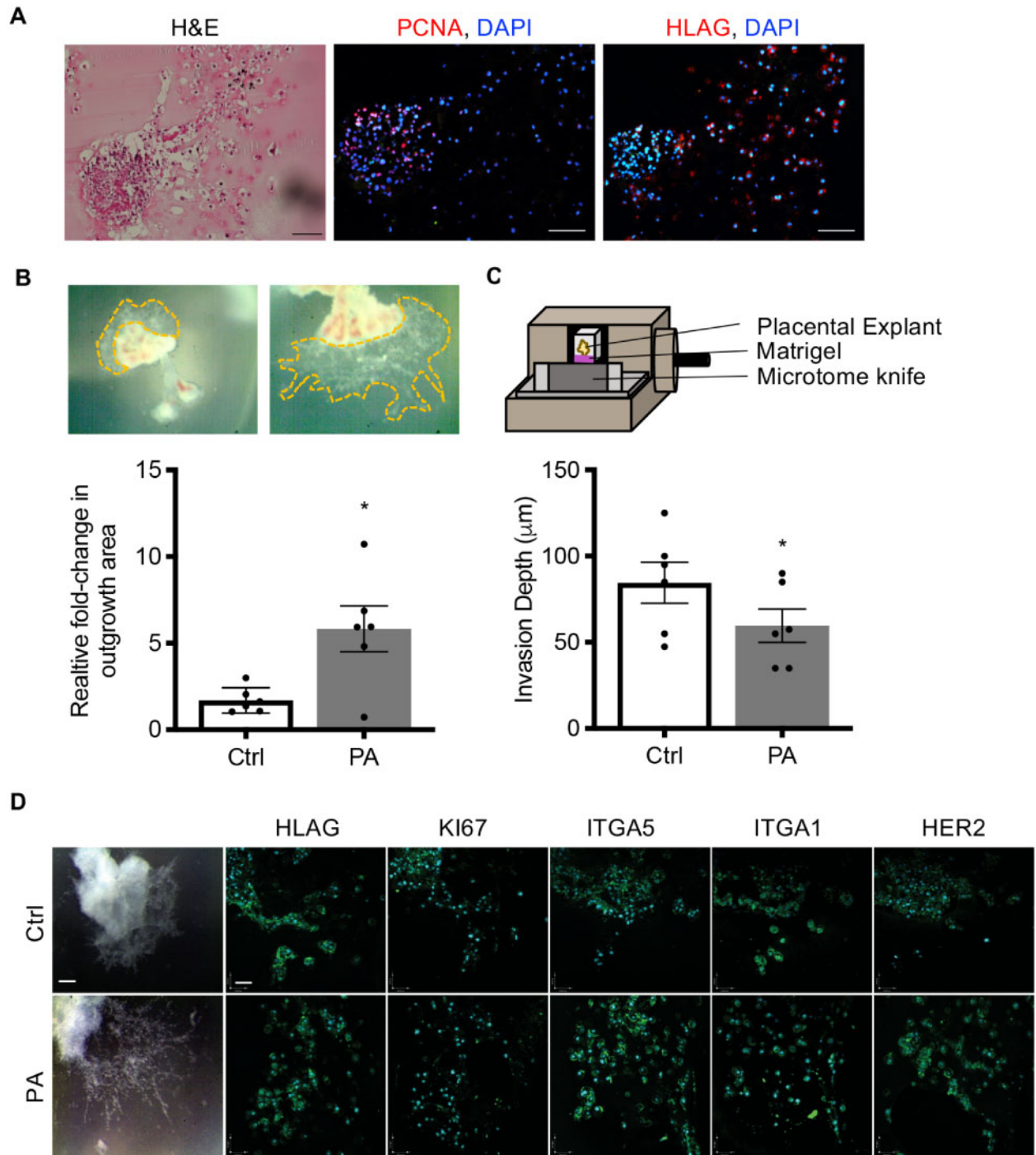


Figure 7. Increased outgrowth and impaired EVT invasion in first trimester placental explants exposed to palmitic acid. (A) Eight-week placental explants cultured for 96 h stained with hematoxylin and eosin (H&E), proliferating cell nuclear antigen (PCNA) and human leukocyte antigen-G (HLAG). Nuclei were detected using 4',6-diamidino-2-phenylindole (DAPI). Scale bar = 100 μm . **(B)** Relative change in placental explant outgrowth area after exposure to SMC-conditioned media containing BSA (Ctrl) or 125 μM PA. Representative images of the explants are depicted above the graph. **(C)** Depth of EVT invasion into Matrigel following exposure to SMC-conditioned media containing BSA (Ctrl) or PA. Graphs represent means \pm SEM based on three explants prepared from each of six different placentas. Asterisks denote statistical significance ($*P < 0.05$). **(D)** Placental explants cultured in SMC-conditioned media containing BSA (Ctrl) or PA. Explants are shown in phase-contrast (left panels), or after being sectioned and immunostained using antibodies specific for HLAG (EVT marker), KI67, ITGA5 (proliferating EVTs), ITGA1 and HER2 (invasive EVTs). Nuclei were detected using DAPI. Images are representative of two explants from each of six different placentas. Scale bar of phase images = 300 μm ; scale bar of immunofluorescent images = 50 μm .

concentration of palmitic acid present at the maternal-placental interface during early pregnancy is not known, 125 μM palmitic acid is consistent with other cell culture studies modeling hyperlipidemia seen in obesity and related comorbidities (Benoit et al., 2009; Hua et al., 2015; Jiang et al., 2017; Frommer et al., 2019; Hernández-Cáceres et al., 2019; Zeng et al., 2020). Others have reported compromised trophoblast viability following exposure to high doses of palmitic acid, including endoplasmic reticulum stress, proliferation defects, and reduced viability in HTR8 EVT cells exposed to 400 and 800 μM palmitic acid, as well as lipotoxicity in human syncytiotrophoblast exposed to 200 and 400 μM palmitic acid (Colvin et al., 2017; Yang et al., 2018). Our study is the first to show the effect of palmitic acid on EVT motility at sublethal doses. Palmitic acid can either stimulate (Chung et al., 2012; Balaban et al., 2017; Landim et al., 2018) or inhibit (Trombetta et al., 2013; Girona et al., 2019) migration of distinct cell-types, suggesting that the impact of palmitic acid on cell motility is likely dose, cell-type and context-specific. We found that palmitic acid attenuated migration and invasion of HTR8 EVT cells, and reduced EVT invasion in first trimester placental explants, whereas there was no effect on EVT motility when cells were exposed to an unsaturated fatty acid, oleic acid. Furthermore, palmitic acid induced expression of several genes encoding inflammatory (*IL6*, *CXCL8*), vasoactive (*EDNI*) and fibrogenic (*SERPINE1*) proteins, all of which are increased in serum of obese patients (Alessi et al., 2000; Derosa et al., 2013) and in various pregnancy complications (Raghupathy, 2013; Ye et al., 2017). High levels of palmitic acid in susceptible pregnancies may therefore contribute to a suboptimal microenvironment at the maternal-placental interface that impairs EVT motility and predisposes to deficient placentation.

In the current study, we detected elevated levels of PAII in women with early-onset preeclampsia compared to age-matched controls, which is consistent with several other studies (Purwosunu et al., 2007; Wikström et al., 2009; Bodova et al., 2011). Unfortunately, we did not have patient consent to obtain additional information such as BMI or palmitic acid concentrations in blood, so correlating these parameters with PAII concentrations is the subject of future investigations. High levels of PAII may impede placental development by promoting occlusive lesions and deposition of fibrin within placental vasculature (Estellés et al., 1994), as well as restricting EVT migration by inhibiting degradation of extracellular matrices (Floridon et al., 2000; Renaud et al., 2005; Lash et al., 2006). Conversely, low expression of PAII is associated with uncontrolled trophoblast invasion in molar pregnancies (Floridon et al., 2000). In the current study, treatment of HTR8 EVT cells with palmitic acid increased PAII expression. Palmitic acid induces PAII in other cell-types (e.g. renal epithelial cells), indicating that high circulating levels of palmitic acid may enhance PAII production by many tissues, resulting in elevated systemic levels of this protein (Jeong et al., 2016). We found that knocking down expression of PAII did not affect migration or invasion of EVT cells in control conditions, which we attribute to EVT cells already migrating at high capacity. Intriguingly, when EVT cells were exposed to palmitic acid, motility was abrogated in control cells but completely restored in PAII-deficient cells. Antibody-mediated neutralization of PAII also rescues EVT migration following exposure to the pro-inflammatory cytokine tumor necrosis factor alpha (Bauer et al., 2004). Increased PAII levels may therefore contribute to poor EVT migration and deficient placentation in various pathophysiological conditions, such as in pregnancies with high plasma levels of palmitic acid or inflammatory cytokines.

In sum, our findings show that EVT migration is stimulated by SMCs, and that palmitic acid interferes with this process. We recognize that palmitic acid is only one factor of many circulating at aberrant levels in blood of patients with metabolic disturbances such as obesity that may influence EVT gene expression signatures and migratory phenotypes. However, palmitic acid is the most common saturated fatty acid circulating in human blood (Carta et al., 2017), and our data show that it is sufficient to induce inflammatory and fibrogenic mediators in EVT cells. Thus, altered levels of this particular fatty acid may have major impacts on trophoblast function and placental development. We exploited HTR8 EVT cells for analysis of PAII expression and knockdown since these cells are advantageous as models of migratory first trimester EVT cells and are amenable to stable incorporation of shRNAs. Although technical limitations precluded us from using shRNA to disrupt PAII expression in placental explants, in future studies it would be interesting to determine whether neutralization of PAII, via recently developed pharmacological inhibitors (Placencio et al., 2015), is sufficient to restore EVT invasion following exposure to palmitic acid. Our findings are in support of others (Seferovic and Gupta, 2016), who suggest that monitoring PAII levels may have diagnostic utility as a biomarker to predict placental insufficiency. Furthermore, our study opens doors to new therapeutic interventions in which managing levels of palmitic acid or PAII to within a 'normal' physiological range may help to restore trophoblast function and prevent dysfunctional placentation. Considering the current prevalence of obesity in women of child-bearing age, this intervention may be useful in reducing the high risk of adverse pregnancy outcomes common to obese pregnancies.

Supplementary data

Supplementary data are available at *Molecular Human Reproduction* online.

Acknowledgements

The authors wish to thank Peeyush Lala (University of Western Ontario) for providing HTR8 EVT cells; and Kristin Chadwick and Dendra Hillier (University of Western Ontario) for technical support. The authors thank the donors, the Research Centre for Women's and Infants' Health BioBank Program at the Lunenfeld-Tanenbaum Research Institute, and the Mount Sinai Hospital and University Hospital Network Department of Obstetrics and Gynecology for the human specimens used in this study.

Data availability

The data underlying this article are available in the article and in its online [supplementary material](#).

Authors' roles

A.M.R. and S.J.R. contributed to the overall approach and design of experiments. A.M.R. conducted all experiments involving cell lines. Experiments involving explants were designed and conducted by

A.M.R., C.E.D. and S.J.L. A.M.R. and S.J.R. wrote the manuscript. All authors critically revised the manuscript and approved the final version.

Funding

This study was funded through grants awarded from the Canadian Institutes of Health Research (PJT152983 and MY3-155368) and Children's Health Research Institute (London, Canada) to S.J.R., with personnel support from the Natural Sciences and Engineering Research Council of Canada (05053) and the Ontario Early Researcher Awards (ER17-13-172). A.M.R. was supported, in part, by a fellowship from the Children's Health Research Institute. C.E.D. and S.J.L. were supported by a foundation award from CIHR FDN143262.

Conflict of interest

The authors declare no conflict of interest.

References

- Alessi MC, Bastelica D, Morange P, Berthet B, Leduc I, Verdier M, Geel O, Juhan-Vague I. Plasminogen activator inhibitor 1, transforming growth factor-beta 1, and BMI are closely associated in human adipose tissue during morbid obesity. *Diabetes* 2000;**49**: 1374–1380.
- Åmark H, Westgren M, Persson M. Prediction of stillbirth in women with overweight or obesity—a register-based cohort study. *PLoS One* 2018;**13**:e0206940.
- Avagliano L, Bulfamante GP, Morabito A, Marconi AM. Abnormal spiral artery remodelling in the decidual segment during pregnancy: from histology to clinical correlation. *J Clin Pathol* 2011;**64**: 1064–1068.
- Avagliano L, Marconi AM, Romagnoli S, Bulfamante GP. Abnormal spiral arteries modification in stillbirths: the role of maternal pre-pregnancy body mass index. *J Matern Fetal Neonatal Med* 2012;**25**: 2789–2792.
- Baines KJ, Rampersaud AM, Hillier DM, Jeyarajah MJ, Grafham GK, Eastbrook G, Laceyfield JC, Renaud SJ. Antiviral inflammation during early pregnancy reduces placental and fetal growth trajectories. *J Immunol* 2020;**204**:694–706.
- Balaban S, Shearer RF, Lee LS, Geldermalsen M, van Schreuder M, Shtein HC, Cairns R, Thomas KC, Fazakerley DJ, Grewal T et al. Adipocyte lipolysis links obesity to breast cancer growth: adipocyte-derived fatty acids drive breast cancer cell proliferation and migration. *Cancer Metab* 2017;**5**:1.
- Bauer S, Pollheimer J, Hartmann J, Husslein P, Aplin JD, Knöfler M. Tumor necrosis factor-alpha inhibits trophoblast migration through elevation of plasminogen activator inhibitor-1 in first-trimester villos explant cultures. *J Clin Endocrinol Metab* 2004;**89**:812–822.
- Benoit SC, Kemp CJ, Elias CF, Abplanalp W, Herman JP, Migrenne S, Lefevre A-L, Cruciani-Guglielmacci C, Magnan C, Yu F et al. Palmitic acid mediates hypothalamic insulin resistance by altering PKC-theta subcellular localization in rodents. *J Clin Invest* 2009;**119**:2577–2589.
- Boden G. Obesity and free fatty acids. *Endocrinol Metab Clin North Am* 2008;**37**:635–646, viii–ix.
- Bodova KB, Biringir K, Dokus K, Ivankova J, Stasko J, Danko J. Fibronectin, plasminogen activator inhibitor type 1 (PAI-1) and uterine artery Doppler velocimetry as markers of preeclampsia. *Dis Markers* 2011;**30**:191–196.
- Bolnick AD, Bolnick JM, Kohan-Ghadr H-R, Kilburn BA, Pasalodos OJ, Singhal PK, Dai J, Diamond MP, Armant DR, Drewlo S. Enhancement of trophoblast differentiation and survival by low molecular weight heparin requires heparin-binding EGF-like growth factor. *Hum Reprod* 2017;**32**:1218–1229.
- Bulmer JN, Innes BA, Levey J, Robson SC, Lash GE. The role of vascular smooth muscle cell apoptosis and migration during uterine spiral artery remodeling in normal human pregnancy. *FASEB J* 2012;**26**:2975–2985.
- Carta G, Murru E, Banni S, Manca C. Palmitic acid: physiological role, metabolism and nutritional implications. *Front Physiol* 2017;**8**:902.
- Challier JC, Basu S, Bintein T, Minium J, Hotmire K, Catalano PM, Hauguel-de Mouzon S. Obesity in pregnancy stimulates macrophage accumulation and inflammation in the placenta. *Placenta* 2008;**29**:274–281.
- Chen X, Scholl TO, Leskiw M, Savaille J, Stein TP. Differences in maternal circulating fatty acid composition and dietary fat intake in women with gestational diabetes mellitus or mild gestational hyperglycemia. *Diabetes Care* 2010;**33**:2049–2054.
- Chung JH, Jeon HJ, Hong S-Y, Lee DL, Lee KH, Kim SH, Han YS, Manabe I, Miller YI, Lee S-H. Palmitate promotes the paracrine effects of macrophages on vascular smooth muscle cells: the role of bone morphogenetic proteins. *PLoS One* 2012;**7**:e29100.
- Colvin BN, Longtine MS, Chen B, Costa ML, Nelson DM. Oleate attenuates palmitate-induced endoplasmic reticulum stress and apoptosis in placental trophoblasts. *Reproduction* 2017;**153**:369–380.
- Cotecchini T, Graham CH. Aberrant maternal inflammation as a cause of pregnancy complications: a potential therapeutic target? *Placenta* 2015;**36**:960–966.
- Damsky CH, Librach C, Lim KH, Fitzgerald ML, McMaster MT, Janatpour M, Zhou Y, Logan SK, Fisher SJ. Integrin switching regulates normal trophoblast invasion. *Development* 1994;**120**: 3657–3666.
- Derosa G, Fogari E, D'Angelo A, Bianchi L, Bonaventura A, Romano D, Maffioli P. Adipocytokine levels in obese and non-obese subjects: an observational study. *Inflammation* 2013;**36**:914–920.
- Estellés A, Gilabert J, Keeton M, Eguchi Y, Aznar J, Grancha S, España F, Loskutoff DJ, Schleaf RR. Altered expression of plasminogen activator inhibitor type 1 in placentas from pregnant women with preeclampsia and/or intrauterine fetal growth retardation. *Blood* 1994;**84**:143–150.
- Floridon C, Nielsen O, Hølund B, Sweep F, Sunde L, Thomsen SG, Teisner B. Does plasminogen activator inhibitor-1 (PAI-1) control trophoblast invasion? A study of fetal and maternal tissue in intra-uterine, tubal and molar pregnancies. *Placenta* 2000;**21**:754–762.
- Frommer KW, Hasseli R, Schäffler A, Lange U, Rehart S, Steinmeyer J, Rickert M, Sarter K, Zaiss MM, Culmsee C. Free fatty acids in bone pathophysiology of rheumatic diseases. *Front Immunol* 2019;**10**:2757.
- Girona J, Rosales R, Saavedra P, Masana L, Vallvé J-C. Palmitate decreases migration and proliferation and increases oxidative stress

- and inflammation in smooth muscle cells: role of the Nrf2 signaling pathway. *Am J Physiol Cell Physiol* 2019;**316**:C888–C897.
- Graham CH, Hawley TS, Hawley RG, MacDougall JR, Kerbel RS, Khoo N, Lala PK. Establishment and characterization of first trimester human trophoblast cells with extended lifespan. *Exp Cell Res* 1993;**206**:204–211.
- Gupta S, Knight AG, Gupta S, Keller JN, Bruce-Keller AJ. Saturated long-chain fatty acids activate inflammatory signaling in astrocytes. *J Neurochem* 2012;**120**:1060–1071.
- Han J, Li L, Hu J, Yu L, Zheng Y, Guo J, Zheng X, Yi P, Zhou Y. Epidermal growth factor stimulates human trophoblast cell migration through Rho A and Rho C activation. *Endocrinology* 2010;**151**:1732–1742.
- Harris LK, Keogh RJ, Wareing M, Baker PN, Cartwright JE, Aplin JD, Whitley GSJ. Invasive trophoblasts stimulate vascular smooth muscle cell apoptosis by a fas ligand-dependent mechanism. *Am J Pathol* 2006;**169**:1863–1874.
- Hayes EK, Tessier DR, Percival ME, Holloway AC, Petrik JJ, Gruslin A, Raha S. Trophoblast invasion and blood vessel remodeling are altered in a rat model of lifelong maternal obesity. *Reprod Sci* 2014;**21**:648–657.
- Hernández-Cáceres MP, Toledo-Valenzuela L, Díaz-Castro F, Ávalos Y, Burgos P, Narro C, Peña-Oyarzun D, Espinoza-Cacedo J, Cifuentes-Araneda F, Navarro-Aguad F et al. Palmitic acid reduces the autophagic flux and insulin sensitivity through the activation of the free fatty acid receptor 1 (FFAR1) in the hypothalamic neuronal cell line N43/5. *Front Endocrinol (Lausanne)* 2019;**10**:176.
- Hua W, Huang H, Tan L, Wan J, Gui H, Zhao L, Ruan X, Chen X, Du X. CD36 mediated fatty acid-induced podocyte apoptosis via oxidative stress. *PLoS One* 2015;**10**:e0127507.
- Jaju Bhattad G, Jeyarajah MJ, McGill MG, Dumeaux V, Okae H, Arima T, Lajoie P, Bérubé NG, Renaud SJ. Histone deacetylase 1 and 2 drive differentiation and fusion of progenitor cells in human placental trophoblasts. *Cell Death Dis* 2020;**11**:311.
- James JL, Cartwright JE, Whitley GS, Greenhill DR, Hoppe A. The regulation of trophoblast migration across endothelial cells by low shear stress: consequences for vascular remodelling in pregnancy. *Cardiovasc Res* 2012;**93**:152–161.
- Jensen MD, Haymond MW, Rizza RA, Cryer PE, Miles JM. Influence of body fat distribution on free fatty acid metabolism in obesity. *J Clin Invest* 1989;**83**:1168–1173.
- Jeong BY, Uddin MJ, Park JH, Lee JH, Lee HB, Miyata T, Ha H. Novel plasminogen activator inhibitor-1 inhibitors prevent diabetic kidney injury in a mouse model. *PLoS One* 2016;**11**:e0157012.
- Jeyarajah MJ, Jaju Bhattad G, Kops BF, Renaud SJ. Syndecan-4 regulates extravillous trophoblast migration by coordinating protein kinase C activation. *Sci Rep* 2019;**9**:10175.
- Jiang X-S, Chen X-M, Wan J-M, Gui H-B, Ruan X-Z, Du X-G. Autophagy protects against palmitic acid-induced apoptosis in podocytes *in vitro*. *Sci Rep* 2017;**7**:42764.
- Korbecki J, Bajdak-Rusinek K. The effect of palmitic acid on inflammatory response in macrophages: an overview of molecular mechanisms. *Inflamm Res* 2019;**68**:915–932.
- Landim BC, Jesus MM, de Bosque BP, Zanon RG, Silva CV, da Góes RM, Ribeiro DL. Stimulating effect of palmitate and insulin on cell migration and proliferation in PNT1A and PC3 prostate cells: counteracting role of metformin. *Prostate* 2018;**78**:731–742.
- Lash GE, Otun HA, Innes BA, Bulmer JN, Searle RF, Robson SC. Low oxygen concentrations inhibit trophoblast cell invasion from early gestation placental explants via alterations in levels of the urokinase plasminogen activator system. *Biol Reprod* 2006;**74**:403–409.
- Leddy MA, Power ML, Schulkin J. The impact of maternal obesity on maternal and fetal health. *Rev Obstet Gynecol* 2008;**1**:170–178.
- Lyll F, Robson SC, Bulmer JN. Spiral artery remodeling and trophoblast invasion in preeclampsia and fetal growth restriction: relationship to clinical outcome. *Hypertension* 2013;**62**:1046–1054.
- Lynch CM, Sexton DJ, Hession M, Morrison JJ. Obesity and mode of delivery in primigravid and multigravid women. *Amer J Perinatol* 2008;**25**:163–167.
- Mavri A, Stegnar M, Krebs M, Sentocnik JT, Geiger M, Binder BR. Impact of adipose tissue on plasma plasminogen activator inhibitor-1 in dieting obese women. *Arterioscler Thromb Vasc Biol* 1999;**19**:1582–1587.
- Moser G, Windsperger K, Pollheimer J, de Sousa Lopes SC, Huppertz B. Human trophoblast invasion: new and unexpected routes and functions. *Histochem Cell Biol* 2018;**150**:361–370.
- Myatt L, Maloyan A. Obesity and placental function. *Semin Reprod Med* 2016;**34**:42–49.
- Nadeem L, Munir S, Fu G, Dunk C, Baczyk D, Caniggia I, Lye S, Peng C. Nodal signals through activin receptor-like kinase 7 to inhibit trophoblast migration and invasion: implication in the pathogenesis of preeclampsia. *Am J Pathol* 2011;**178**:1177–1189.
- Placencio VR, Ichimura A, Miyata T, DeClerck YA. Small molecule inhibitors of plasminogen activator inhibitor-1 elicit anti-tumorigenic and anti-angiogenic activity. *PLoS One* 2015;**10**:e0133786.
- Purwosunu Y, Sekizawa A, Koide K, Farina A, Wibowo N, Wiknosastro GH, Okazaki S, Chiba H, Okai T. Cell-free mRNA concentrations of plasminogen activator inhibitor-1 and tissue-type plasminogen activator are increased in the plasma of pregnant women with preeclampsia. *Clin Chem* 2007;**53**:399–404.
- Raghupathy R. Cytokines as key players in the pathophysiology of preeclampsia. *Med Princ Pract* 2013;**22**:8–19.
- Renaud SJ, Cotechini T, Quirt JS, Macdonald-Goodfellow SK, Othman M, Graham CH. Spontaneous pregnancy loss mediated by abnormal maternal inflammation in rats is linked to deficient uteroplacental perfusion. *J Immunol* 2011;**186**:1799–1808.
- Renaud SJ, Kubota K, Rumi MAK, Soares MJ. The FOS transcription factor family differentially controls trophoblast migration and invasion. *J Biol Chem* 2014;**289**:5025–5039.
- Renaud SJ, Postovit L-M, Macdonald-Goodfellow SK, McDonald GT, Caldwell JD, Graham CH. Activated macrophages inhibit human cytotrophoblast invasiveness *in vitro*. *Biol Reprod* 2005;**73**:237–243.
- Roberts JM, Bodnar LM, Patrick TE, Powers RW. The role of obesity in preeclampsia. *Pregnancy Hypertens* 2011;**1**:6–16.
- Salomon C, Yee S, Scholz-Romero K, Kobayashi M, Vaswani K, Kvaskoff D, Illanes SE, Mitchell MD, Rice GE. Extravillous trophoblast cells-derived exosomes promote vascular smooth muscle cell migration. *Front Pharmacol* 2014;**5**:175.
- Schneider CA, Rasband WS, Eliceiri KW. NIH Image to ImageJ: 25 years of image analysis. *Nat Methods* 2012;**9**:671–675.

- Seferovic MD, Gupta MB. Increased umbilical cord PAI-1 levels in placental insufficiency are associated with fetal hypoxia and angiogenesis. *Dis Markers* 2016;**2016**:7124186.
- Sergi D, Morris AC, Kahn DE, McLean FH, Hay EA, Kubitz P, MacKenzie A, Martinoli MG, Drew JE, Williams LM. Palmitic acid triggers inflammatory responses in N42 cultured hypothalamic cells partially via ceramide synthesis but not via TLR4. *Nutr Neurosci* 2020;**23**:321–334.
- Silva JF, Serakides R. Intrauterine trophoblast migration: a comparative view of humans and rodents. *Cell Adh Migr* 2016;**10**:88–110.
- Tian H, Liu C, Zou X, Wu W, Zhang C, Yuan D. MiRNA-194 regulates palmitic acid-induced toll-like receptor 4 inflammatory responses in THP-1 cells. *Nutrients* 2015;**7**:3483–3496.
- Trombetta A, Togliatto G, Rosso A, Dentelli P, Olgasi C, Cotogni P, Brizzi MF. Increase of palmitic acid concentration impairs endothelial progenitor cell and bone marrow-derived progenitor cell bioavailability: role of the STAT5/PPAR γ transcriptional complex. *Diabetes* 2013;**62**:1245–1257.
- Vidakovic AJ, Jaddoe VVV, Gishti O, Felix JF, Williams MA, Hofman A, Demmelmair H, Koletzko B, Tiemeier H, Gaillard R. Body mass index, gestational weight gain and fatty acid concentrations during pregnancy: the Generation R Study. *Eur J Epidemiol* 2015;**30**:1175–1185.
- Whitley GSJ, Cartwright JE. Trophoblast-mediated spiral artery remodelling: a role for apoptosis. *J Anat* 2009;**215**:21–26.
- Wikström A-K, Nash P, Eriksson UJ, Olovsson MH. Evidence of increased oxidative stress and a change in the plasminogen activator inhibitor (PAI)-1 to PAI-2 ratio in early-onset but not late-onset preeclampsia. *Am J Obstet Gynecol* 2009;**201**:597.e1–8.
- Wright JK, Dunk CE, Amsalem H, Maxwell C, Keating S, Lye SJ. HER1 signaling mediates extravillous trophoblast differentiation in humans. *Biol Reprod* 2010;**83**:1036–1045.
- Yang C, Lim W, Bazer FW, Song G. Down-regulation of stearoyl-CoA desaturase-1 increases susceptibility to palmitic-acid-induced lipotoxicity in human trophoblast cells. *J Nutr Biochem* 2018;**54**:35–47.
- Yang X, Haghiaç M, Glazebrook P, Minium J, Catalano PM, Hauguel-de Mouzon S. Saturated fatty acids enhance TLR4 immune pathways in human trophoblasts. *Hum Reprod* 2015;**30**:2152–2159.
- Ye Y, Vattai A, Zhang X, Zhu J, Thaler CJ, Mahner S, Jeschke U, von Schönfeldt V. Role of plasminogen activator inhibitor type 1 in pathologies of female reproductive diseases. *Int J Mol Sci* 2017;**18**:1651.
- Yew Tan C, Virtue S, Murfitt S, Roberts LD, Phua YH, Dale M, Griffin JL, Tinahones F, Scherer PE, Vidal-Puig A. Adipose tissue fatty acid chain length and mono-unsaturation increases with obesity and insulin resistance. *Sci Rep* 2015;**5**:18366.
- Zeng X, Zhu M, Liu X, Chen X, Yuan Y, Li L, Liu J, Lu Y, Cheng J, Chen Y. Oleic acid ameliorates palmitic acid induced hepatocellular lipotoxicity by inhibition of ER stress and pyroptosis. *Nutr Metab (Lond)* 2020;**17**:11.
- Zhou B, Zhang J, Zhang Q, Permatasari F, Xu Y, Wu D, Yin Z, Luo D. Palmitic acid induces production of proinflammatory cytokines interleukin-6, interleukin-1 β , and tumor necrosis factor- α via a NF- κ B-dependent mechanism in HaCaT keratinocytes. *Mediators Inflamm* 2013;**2013**:530429.